Food Biophysics (2026) 21:41
https://doi.org/10.1007/s11483-026-10129-5

RESEARCH

Mechanistic Insights into the Biological Effects of *Aronia melanocarpa* Through *In vitro* Assays, Molecular Docking and Bioinformatic Analysis

Cansu Öztürk[1] · Songül Bayrak[1] · Şeyda Nur Kalın[2] · Namık Kılınç[3] · Yeliz Demir[1,4] · Ömer İrfan Küfrevioğlu[1]

Received: 14 February 2026 / Accepted: 20 March 2026
© The Author(s) 2026

Abstract

Aronia melanocarpa is recognized to be a polyphenol-rich fruit with promising bioactivities; however, there are limited multidisciplinary analyses of it using both experimental and computational analyses. The current study critically investigated aqueous (AWE) and ethanolic (AEE) extracts of *A. melanocarpa* grown in Turkey that defined their phytochemical composition and biological relevance via *in vitro*, *in silico*, and bioinformatics studies. LCMS/MS quantitatively determined quinic acid, cyanidin-3-O-glucoside and chlorogenic acid as the most prevalent phenolic compounds in both extracts. The two extracts showed strong antioxidant activity in a range of methods (DPPH, ABTS, FRAP, CUPRAC, and metal-reducing) with AEE always showing better performance and coming close to the established standard antioxidants. The extracts had strong inhibition of therapeutic enzymes including acetylcholinesterase, alpha-glucosidase, and human carbonic anhydrase I-II which was better than the inhibitors. Antimicrobial testing showed a broad-spectrum antibacterial activity, which was indicated by low minimal inhibitory concentration, especially of the ethanolic extract. Cytotoxicity profiling also revealed that AEE had a selective antiproliferative effect on A549 lung cancer cells and a limited response in MCF-7 breast cancer cells. Cyanidin-3 -O -glucoside was identified as the leading contributor to the enzyme inhibition activity by induced -fit molecular docking studies. Furthermore, bioinformatic enrichment studies linked molecular targets that were predicted with pathways related to the oxidative stress, metabolic regulation, inflammation, and cell survival. These findings demonstrate that *A. melanocarpa* exerts its biological effects through multi-target and network-level mechanisms, supporting its potential as a functional food.

Keywords Aronia · Anticancer · Antioxidant · LC–MS/MS · Inhibition · Molecular docking · Bioinformatic

Introduction

In recent years, increasing attention has been directed toward foods that provide health benefits beyond basic nutrition, particularly those rich in bioactive phytochemicals [1]. Among these, berries have emerged as prominent functional foods due to their low caloric content and high concentrations of polyphenols, flavonoids, and anthocyanins [2]. These compounds are widely recognized for their antioxidant capacity and their ability to modulate oxidative stress, inflammation, and cellular damage, which are central mechanisms underlying the development of chronic metabolic and degenerative diseases [3]. The major anthocyanins present in *Aronia melanocarpa* extracts, particularly cyanidin and its glycosides, have been reported to exhibit pronounced anti-inflammatory activity [4]. In particular, metabolites of cyanidin-3-glucoside, the predominant anthocyanin in aronia, have been shown to significantly

✉ Cansu Öztürk
cansu_36_25@hotmail.com

✉ Yeliz Demir
yelizdemir2116@gmail.com; yelizdemir@ardahan.edu.tr

[1] Department of Chemistry, Faculty of Science, Atatürk University, 25240 Erzurum, Türkiye

[2] Department of Molecular Biology and Genetics, Faculty of Science, Atatürk University, 25240 Erzurum, Türkiye

[3] Department of Medical Services and Techniques, Vocational School of Health Services, Igdır University, 76000 Igdır, Türkiye

[4] Department of Pharmacy Services, Nihat Delibalta Göle Vocational High School, Ardahan University, Ardahan, Türkiye

Published online: 10 April 2026

reduce the expression of inflammatory mediators, including IL-6, in human vascular cells [5]. Epidemiological and experimental studies consistently suggest that diets enriched with anthocyanin-rich fruits are associated with reduced risks of cardiovascular diseases, type 2 diabetes, neurodegenerative disorders, and certain cancers [6, 7].

Within this context, black chokeberry (*A. melanocarpa*) has gained particular scientific interest owing to its exceptionally high polyphenol content and broad spectrum of reported biological activities [8]. It is also important to emphasize the distinctive position of *A. melanocarpa* among berry fruits. The total polyphenol content of aronia has been reported to exceed that of several widely consumed berries, including blueberries, raspberries, strawberries, and blackberries. This exceptionally high phenolic concentration is considered one of the main factors underlying the pronounced biological and antioxidant activities attributed to aronia [9].

The fruit is a rich source of phenolic acids (notably caffeoylquinic acids), anthocyanins, flavonols, and proanthocyanidins, which collectively confer strong antioxidant potential [10]. Previous studies have linked *A. melanocarpa* consumption to anti-inflammatory, hypoglycemic, cardioprotective, anticoagulant, and antimicrobial effects, highlighting its relevance as a functional food and nutraceutical ingredient [11–14]. In addition to its phytochemical richness, aronia also contains essential sugars, minerals, trace elements, and vitamins, further enhancing its nutritional and technological value for food applications [15, 16].

Beyond its nutritional attributes, aronia extracts have attracted attention for their potential role in food preservation and safety, as their antioxidant and antimicrobial properties may contribute to delaying lipid oxidation and inhibiting microbial growth in food systems [17, 18]. However, it is well established that the biological efficacy of aronia products is strongly influenced by factors such as geographical origin, cultivation conditions, and, critically, the extraction solvent [19]. Different extraction media selectively enrich distinct phenolic subclasses, which in turn can markedly alter functional outcomes [20]. Therefore, understanding the relationship between extraction-dependent phytochemical composition and biological activity remains essential for the rational development of aronia-based functional products.

From a mechanistic perspective, oxidative stress, chronic inflammation, and dysregulated metabolic signaling constitute common pathological pathways shared by metabolic disorders, neurodegenerative diseases, and age-related conditions [21, 22]. Key enzymes involved in these processes including α-glucosidase, acetylcholinesterase (AChE), and human carbonic anhydrase isoenzymes I and II (hCA I–II) are well-established molecular targets in the management of diabetes, neurodegeneration, and ocular or metabolic disorders [23, 24]. Natural inhibitors of these enzymes are increasingly sought as safer alternatives or complements to synthetic drugs, which are often associated with adverse effects during long-term use [25]. Plant-derived phenolics, particularly anthocyanins and flavonoids, have demonstrated promising inhibitory activity against these enzymes, supporting the concept of multi-target modulation through dietary bioactives [26, 27].

Although numerous studies have investigated the antioxidant capacity and phenolic composition of *A. melanocarpa* cultivated in different regions, important gaps remain in the literatüre [28, 29]. In particular, integrated studies that simultaneously evaluate antioxidant activity, antimicrobial effects, enzyme inhibition, and cytotoxic responses, while also providing molecular-level mechanistic support, are still limited. Moreover, the inhibitory potential of aronia extracts against hCA isoenzymes has been scarcely explored, despite the relevance of these enzymes to physiological regulation and disease. Recent advances in computational biology and bioinformatics now allow the prediction of molecular targets and the mapping of bioactive compounds onto biological pathways, offering a systems-level framework to interpret experimental findings [30].

Therefore, the present study aimed to provide a comprehensive and mechanistically supported evaluation of aqueous (AWE) and ethanolic (AEE) extracts of *A. melanocarpa* cultivated in Turkey. The phytochemical profiles of both extracts were quantitatively characterized using LC–MS/MS, followed by *in vitro* assessment of antioxidant, antimicrobial, enzyme inhibitory, and cytotoxic activities. To further elucidate the molecular basis of the observed bioactivities, induced-fit molecular docking was employed to investigate enzyme–ligand interactions of the major phenolic constituents, and bioinformatic enrichment analyses were conducted to link predicted molecular targets with relevant biological pathways. By integrating experimental, computational, and systems-level approaches, this study seeks to advance the understanding of *A. melanocarpa* as a multifunctional functional food and to provide a rational framework for its future application in food, nutraceutical, and health-related contexts.

Materials and Methods

Chemicals

Analytical standards and reagents (DPPH, ABTS, neocuproine, Trolox, Folin–Ciocalteu reagent, Ellman's reagent/DTNB, etc.) and LC–MS/MS reference phenolics were obtained from Sigma-Aldrich (Steinheim, Germany).

Enzymes used in inhibition assays (AChE from *Electrophorus electricus* and α-glycosidase from baker's yeast) were sourced from Sigma-Aldrich. Bacterial strains (*Bacillus subtilis* ATCC 6633, *Staphylococcus aureus* ATCC 25923, *Escherichia coli* ATCC 43895, *Klebsiella pneumoniae* ATCC 13883) were obtained from the Atatürk University Microbiology Laboratory collection. Additional chemicals were purchased from Sigma-Aldrich or Merck (Darmstadt, Germany). In cell culture studies, human breast cancer (MCF-7) and human non-small cell lung cancer (A549) cell lines were obtained from the American Type Culture Collection (ATCC, USA). Dulbecco's Modified Eagle Medium (DMEM; EcoTech, Turkey), Roswell Park Memorial Institute medium (RPMI-1640; Thermo Fisher Scientific, USA), fetal bovine serum (FBS; HyClone, USA), penicillin/streptomycin (Sigma-Aldrich, USA), and L-glutamine (Gibco™, USA) were used as cell culture media compositions.

Preparation of Plant Extracts

The plant material consisted of dried fruits of black chokeberry (*A. melanocarpa*) purchased from Yalova Province, Türkiye. Dried plant material (10 g) was ground to a particle size of approximately 0.5–1.0 mm. For the ethanolic extract (AEE), the sample was stirred with 50 mL of ethanol for 5 h. In the case of the aqueous extract (AWE), we used 50 mL of distilled water and extracted overnight. The filtrate was centrifuged at 3000 rpm for 10 min The supernatants were subsequently filtered through cheesecloth followed by Whatman No. 1 filter paper. Rotary evaporation was used to remove ethanol; water was dried using lyophilization to get dry extracts. The yield was determined as a percentage of the original dry weight. For LC–MS/MS analysis, 100 mg of each dry extract was dissolved in an appropriate solvent [31].

Phytochemical Characterization

Total Phenolic Content (TPC)

TPC was determined using a modified Folin–Ciocalteu method. Extract (0.5 mL; 1 mg/mL) was mixed with Folin–Ciocalteu reagent (1 mL) and 1% Na_2CO_3 (1 mL), incubated 2 h at room temperature in the dark, and read at 760 nm. Results were expressed as gallic acid equivalents (GAE) using a gallic acid calibration (1–200 µg/mL) [32].

Total Flavonoid Content (TFC)

TFC was measured by an $Al(NO_3)_3$-based colorimetric method. Sample (0.5 mL; 10–30 µg/mL) was mixed with 95% methanol (1.5 mL), potassium acetate (0.5 mL; 1.0 M), distilled water (2.3 mL), and 10% aluminum nitrate (1.5 mL). After 40 min at 25 °C, absorbance was recorded at 415 nm. Results were expressed as quercetin equivalents (QE) using quercetin calibration (1–500 µg/mL) [33].

Reducing Sugar Content

Reducing sugars were quantified by the DNS method. Equal volumes of sample and DNS reagent were incubated at 90 °C for 10 min, cooled, diluted with distilled water, and read at 546 nm. Maltose (1–20 mg/mL) was used for calibration [34].

LC–MS/MS Profiling of Phenolics/Flavonoids

Phenolic and organic acid profiling (35 target analytes) was performed using UHPLC (Agilent 1290 Infinity) coupled to ESI-MS/MS (Agilent 6460) according to a validated method [35]. The extraction durations used in this study (overnight for AWE and 5 h for AEE) were selected based on previously reported protocols to ensure efficient recovery of phenolic compounds. Separation used a Zorbax SB-C18 column (4.6 × 100 mm, 3.5 µm) with water/acetonitrile (each 0.1% formic acid) at 30 °C. A total of 35 phenolic and organic acid compounds were screened using the LC–MS/MS method; however, only the compounds detected above the limit of quantification were reported in the results section. Quantification was conducted in MRM mode with optimized transitions and collision energies. Key instrument settings included drying gas 350 °C (12 L/min), nebulizer 55 psi, sheath gas 250 °C (5 L/min), capillary voltage 3.5 kV. Data were processed using Agilent MassHunter [36]. Quantitative analysis was performed using external calibration curves prepared from authentic reference standards. Calibration curves were constructed at seven concentration levels (100, 250, 500, 750, 1000, 1500, and 2000 µg/mL). Linear regression analysis was applied to establish the relationship between peak area and analyte concentration, and correlation coefficients (R^2) were calculated to evaluate linearity. Detailed calibration curves and corresponding calibration data are provided in the Supplementary Material (Figures S1–S10 and Tables S1–S10). Quantitative results are expressed as ng/mL based on the LC–MS/MS calibration.

Antioxidant Activity

Radical Scavenging Assays

DPPH scavenging was assessed by incubating extract solutions at concentrations of 10, 20, and 30 µg/mL with DPPH for 30 min in the dark and measuring absorbance at 517

nm [37]. The results presented in this study correspond to the highest concentration (30 µg/mL). ABTS radical scavenging was determined using the $ABTS^{\bullet+}$ decolorization approach in line with the referenced protocol, also evaluated at 10, 20, and 30 µg/mL, with results reported for 30 µg/mL. All radical scavenging assays were performed in triplicate ($n = 3$), and results are expressed as mean ± standard deviation (SD).

Reducing Power Assays

Reducing capacity was evaluated by Fe^{3+}-reducing power using phosphate buffer and potassium ferricyanide (incubation at 50 °C for 30 min; absorbance read at 700 nm) [38]. CUPRAC was performed using $CuCl_2$ neocuproine ammonium acetate buffer with absorbance measured at 450 nm after 30 min [39]. FRAP/TPTZ reduction was measured in acetate buffer (pH 3.6) after 30 min at 37 °C with absorbance at 593 nm [40]. All reducing assays were conducted at extract concentrations of 10, 20, and 30 µg/mL, with the data reported for 30 µg/mL, performed in triplicate ($n = 3$) and expressed as mean ± SD.

Determination of Antimicrobial Activity

Disk Diffusion

Bacterial suspensions adjusted to 0.5 McFarland were inoculated onto Mueller–Hinton agar plates. Sterile paper disks impregnated with AEE or AWE (1000 µg/mL, prepared in DMSO/water) were placed on the agar surface. Ampicillin and DMSO were used as positive and negative controls, respectively. After incubation for 24 h at 37 °C, inhibition zone diameters were measured [40].

Microdilution (MIC)

MICs were determined in 96-well plates using Mueller–Hinton broth. Extracts were serially diluted from 1000 to 1.95 µg/mL, inoculated with standardized bacterial culture (0.5 McFarland), incubated 24 h, and growth was assessed by turbidity (600 nm). MIC was recorded as the lowest concentration without visible turbidity [41].

Enzyme Inhibition Studies

AChE Inhibition

AChE inhibition was monitored kinetically at 412 nm for 5 min in 1 M Tris-HCl (pH 8.0) using DTNB (10 mM) and acetylthiocholine iodide (10 mM) as substrate system [42]. Extract concentration was increased stepwise until > 50% inhibition was achieved. Tacrine was used as the reference inhibitor.

hCA I–II Inhibition

hCA I and II were purified from human erythrocytes using Sepharose 4B-L-tyrosine sulfanilamide affinity chromatography [43]. Para-nitrophenyl acetate hydrolysis was followed at 348 nm for 3 min. The reaction (1 mL) contained para-nitrophenyl acetate (0.07 mM), Tris-SO_4 buffer (0.05 M, pH 7.4), and enzyme solution [44]. Extract concentration was increased until > 50% inhibition occurred; acetazolamide served as the positive control.

α-Glucosidase Inhibition

α-Glucosidase inhibition was assessed using p-nitrophenyl-α-D-glucopyranoside (p-NPG) as substrate in 0.1 M phosphate buffer (pH 6.9) following the referenced method [45]. Absorbance was monitored at 405 nm for 5 min. Acarbose was used as the reference inhibitor.

IC_{50} Determination

IC_{50} values were estimated from plots of % enzyme activity versus extract concentration, fitting data to a nonlinear regression model based on increasing inhibitor concentrations.

Cytotoxicity Assay

Cell Culture Condition

MCF-7 cells were maintained in DMEM, while A549 cells were cultured in RPMI-1640. Both media were supplemented with 10% (v/v) heat-inactivated FBS, 1% penicillin/streptomycin, and 1% L-glutamine. Cells were incubated at 37 °C in a humidified atmosphere containing 5% CO_2 [46, 47]. AEE and AWE were dissolved in DMSO (Sigma, USA) to prepare stock solutions (200 mg/mL), which were stored at room temperature until use.

Cell Viability Detection Kit-8 (CVDK-8) Assay

Cells were maintained in culture medium at 37 °C in a humidified atmosphere containing 5% CO_2 and seeded into 96-well plates at a density of 5×10^3 cells per well, followed by overnight attachment. AEE and AWE were diluted in culture medium to final concentrations of 0, 100, 200, 400, 600, 800, and 1000 µg/mL. A solvent control group containing 0.5% DMSO was used as a negative control. Importantly, this negative control did not show a significant difference in

cell viability when compared to the control group (cells cultured in medium only). Cells were subsequently treated with the extracts for 48 h, and the cytotoxic effects were assessed relative to the 0.5% DMSO control group. Cell viability was assessed using the CVDK-8 assay (EcoTech Biotechnology, Türkiye), and absorbance was measured at 450 nm with a microplate reader (BioTek, USA).

In Silico Studies

Induced-Fit Molecular Docking

Induced-fit molecular docking (IFD) simulations were performed to characterize the binding conformations and interaction profiles of quinic acid, cyanidin-3-O-glucoside, and chlorogenic acid within the active sites of AChE, hCAI, hCAII, and α-glycosidase, following an established protocol that accounts for receptor flexibility during ligand accommodation [48]. The computational workflow was designed in accordance with previously validated methodologies reported in related studies [49–51].

All simulations were conducted using Maestro v13.9 within the Schrödinger Molecular Modeling Suite. The X-ray crystallographic structures of AChE (PDB ID: 4TVK) and hCAI (PDB ID: 4WR7), hCAII (PDB ID: 8J2O), and α-glycosidase (PDB ID: 2QMJ) were retrieved from the RCSB Protein Data Bank and subjected to systematic preparation using the Protein Preparation Wizard. This procedure included assignment of bond orders, optimization of hydrogen-bonding networks, determination of protonation states at physiological pH, and restrained energy minimization employing the OPLS4 force field to relieve steric clashes while preserving crystallographic integrity [52–54]. Although the *in vitro* AChE inhibition assays were performed using the enzyme derived from *Electrophorus electricus* (EeAChE), the 3D crystal structure of *Torpedo californica* AChE (TcAChE, PDB ID: 4TVK) was utilized for the molecular docking simulations. TcAChE was selected as a structural surrogate due to its excellent crystallographic resolution and the well-documented, exceptionally high structural conservation of the active site gorge including the catalytic triad and the peripheral anionic site between TcAChE and EeAChE. Therefore, TcAChE serves as a highly reliable and widely accepted model for predicting the binding interactions of EeAChE inhibitors.

Receptor grids were generated by defining the docking region around the centroid of the co-crystallized ligands, thereby ensuring accurate representation of the native binding pockets. To ensure reproducibility, the molecular docking binding pockets were defined based on the native co-crystallized ligands of each target protein. Prior to the docking simulations, the co-crystallized ligands and water molecules were removed from the active sites during the protein preparation step. The grid box was centered on the centroid of each respective native ligand. The grid box dimensions were set to $20 \times 20 \times 20$ Å for all targets to provide a sufficient area for the conformational sampling of the test compounds. The specific grid center coordinates (X, Y, Z) used for each receptor were defined as follows: for 2QMJ (X = -20.79, Y = -6.69, Z = -5.16); for 4TVK (X = -52.45, Y = 30.32, Z = -43.53); for 8J2O (X = 16.51, Y = 3.64, Z = 13.23); and for 4WR7 (X = 11.65, Y = 36.08, Z = 17.05). Ligand structures were prepared using the LigPrep module, where geometries were optimized and ionization states were generated within a pH range of 7.0 ± 2.0 using Epik. The prepared ligands were subsequently docked using the induced-fit protocol, allowing side-chain and backbone flexibility of residues proximal to the binding site to refine protein–ligand complexes and improve binding pose reliability.

Furthermore, the docking protocol was validated by re-docking the native ligands into their respective binding sites. The calculated Root Mean Square Deviation (RMSD) values between the docked poses and the experimental co-crystallized conformations were 1.87 Å for PRD_900007 (alpha-acarbose) in 2QMJ, 0.81 Å for TJH (2-({2-[(6-chloro-1,2,3,4-tetrahydroacridin-9-yl) amino]ethyl}amino)-5-hydroxynaphthalene-1,4-dione) in 4TVK, 1.08 Å for TF9 (acetohexamide) in 8J2O, and 1.17 Å for 3TV (2,3,5,6-tetrafluoro-4-(propylsulfanyl) benzenesulfonamide) in 4WR7. All RMSD values were well below the widely accepted threshold of 2.0 Å, confirming the reliability and accuracy of the utilized docking methodology.

ADME Studies

To evaluate the pharmacokinetic characteristics, drug-likeness, and physicochemical properties of the compounds identified in *A. melanocarpa* extracts, *in silico* ADME analyses were performed. The absorption, distribution, metabolism, and excretion profiles of the investigated compounds were predicted using the QikProp module integrated in Maestro 13.9. This computational platform estimates multiple pharmacokinetic parameters and compares the calculated values with the property ranges reported for approximately 95% of known drugs. Such an approach enables the preliminary assessment of whether the analyzed compounds possess drug-like characteristics and provides useful insights into their potential pharmacokinetic behavior in terms of absorption, distribution, metabolism, and excretion.

Functional Enrichment Analysis

Functional enrichment analysis was performed to explore the biological processes and signaling pathways potentially associated with the predicted molecular targets of the major phenolic compounds identified in *A. melanocarpa* extracts. Target proteins of quinic acid, chlorogenic acid, and cyanidin-3-O-glucoside were first predicted using the SwissTargetPrediction platform with *Homo sapiens* selected as the target organism. After removing duplicate entries and integrating the predicted targets obtained for the three compounds, a combined target list was generated. The UniProt identifiers of the predicted proteins were converted into Entrez Gene IDs using the org.Hs.eg.db annotation database in R (4.5.1) [55]. In total, 240 unique genes were retained and used as the input gene set for subsequent enrichment analyses. Gene Ontology (GO) biological process enrichment, Kyoto Encyclopedia of Genes and Genomes (KEGG) pathway analysis, and Reactome pathway enrichment were performed using the clusterProfiler and ReactomePA packages in R (4.5.1).

To control for multiple testing, p-values were adjusted using the Benjamini–Hochberg false discovery rate (FDR) correction method, and pathways with adjusted p-values below 0.05 were considered statistically significant. It should be noted that enrichment analyses based on small gene sets may occasionally produce unstable statistical signals or inflated enrichment scores due to limited gene representation within certain pathways. However, in the present study, enrichment analyses were conducted using a relatively large integrated gene set ($n = 240$), which reduces potential bias associated with small gene lists and provides a more robust representation of the biological pathways potentially modulated by the phenolic constituents of *A. melanocarpa* extracts.

Statistical Analysis

All experiments were performed in triplicate for each sample, and the results are presented as mean ± standard deviation (SD). The antioxidant activities of both extracts and standard antioxidants were evaluated at different concentrations depending on the assay conditions. In addition, cytotoxic (anticancer) activity experiments were also performed at different concentrations and analyzed using the same statistical approach. Statistical analyses were carried out using GraphPad Prism 5.0 (GraphPad Software, San Diego, CA, USA). Differences among extracts, standard antioxidants, and control groups were analyzed using two-way analysis of variance (ANOVA), followed by Tukey's multiple comparison post-hoc test where appropriate. A p-value of less than 0.05 was considered statistically significant.

Results and Discussion

Phenolic Composition Determined by LC–MS/MS

LC–MS/MS analysis revealed that both ethanolic (AEE) and aqueous (AWE) extracts of *A. melanocarpa* contained high levels of phenolic compounds, with pronounced quantitative differences between the two extraction solvents (Table 1; Fig. 1). Quinic acid was the dominant compound in both extracts, accounting for 45.32% of total phenolics in AEE and 56.48% in AWE, corresponding to concentrations of 54,830.62 ng/mL and 72,480.29 ng/mL extract, respectively. Cyanidin-3-O-glucoside was the second most abundant phenolic, with a notably higher proportion in AEE (40.61%; 49,136.92 ng/mL) compared to AWE (27.42%; 35,192.78 ng/mL). Chlorogenic acid was detected at comparable but slightly higher levels in AWE (15.04%; 19,295.36 ng/mL) than in AEE (13.01%; 15,746.87 ng/mL).

Minor phenolics, including catechin, epicatechin, quercetin, rosmarinic acid, and ellagic acid, were present at substantially lower concentrations but displayed solvent-dependent variability, with flavonoids generally more abundant in AEE. These findings are fully consistent with previous reports identifying caffeoylquinic acids and anthocyanins as the principal phenolic classes in aronia fruits [56, 57]. Importantly, while the qualitative phenolic profile remained conserved across solvents, the quantitative redistribution, particularly the enrichment of anthocyanins and flavonoids in AEE, suggests that extraction polarity plays a decisive role in shaping the functional composition of aronia extracts. This solvent-driven compositional shift provides a mechanistic basis for the differences observed in antioxidant capacity, enzyme inhibition, and antimicrobial activity. These observations further indicate that the biological activities of the extracts are closely related to their phenolic composition. According to the LC–MS/MS results, quinic acid, cyanidin-3-O-glucoside, and chlorogenic acid were identified as the major constituents in both extracts, while other phenolic compounds such as catechin, epicatechin, and quercetin were detected in lower amounts. In particular, anthocyanins such as cyanidin-3-O-glucoside and phenolic acids, including chlorogenic acid, are well known for their antioxidant, antimicrobial, and enzyme-inhibitory properties [58, 59]. Chlorogenic acid has been widely reported to exhibit strong radical scavenging and antimicrobial activities, whereas flavan-3-ols such as catechin and epicatechin contribute to antioxidant capacity through hydrogen-donating and metal-chelating mechanisms [56]. Similarly, flavonols like quercetin are recognized for their potent antioxidant and enzyme-inhibitory effects [60, 61]. Therefore, the relatively high abundance of these phenolic constituents in the extracts may partly account for the pronounced

Table 1 Quantitative determination of phenolic compounds in aronia extracts using LC–MS/MS analysis

No.	Compound	Extract	RT (min)	Response	Concentration (ng/mL)	Yield (%)
1	Quinic acid	AEE	2.344	143,765	54,830.62	45.32
		AWE	2.359	190,016	72,480.29	56.48
2	Cyanidin-3-O-glucoside	AEE	10.394	496,025	49,136.92	40.61
		AWE	10.409	355,191	35,192.78	27.42
3	Keracyanin chloride	AEE	10.509	120	101.04	0.08
		AWE	10.494	358	112.13	0.09
4	Chlorogenic acid	AEE	10.816	415,758	15,746.87	13.01
		AWE	10.802	509,264	19,295.36	15.04
5	Peonidin-3-O-glucoside	AEE	10.915	115	21.16	0.02
		AWE	10.944	39	5.87	0.01
6	Catechin	AEE	11.384	4,553	487.56	0.40
		AWE	11.384	4,110	437.02	0.34
7	Epicatechin	AEE	11.384	4,758	382.19	0.32
		AWE	11.384	4,373	347.91	0.27
8	Ellagic acid	AEE	12.108	313	19.25	0.02
		AWE	12.036	70	<LOD	<LOD
9	Rosmarinic acid	AEE	12.555	279	80.77	0.07
		AWE	12.526	233	69.35	0.05
10	Quercetin	AEE	13.485	10,095	188.33	0.16
		AWE	13.485	18,230	384.67	0.30

Abbreviation:<*LOD* limit of detection

biological activities observed in the present study, which is consistent with previous reports describing the antioxidant and enzyme inhibitory potential of similar phenolic compounds [62, 63].

Antioxidant activity

Total phenolic and flavonoid content analyses confirmed that both extracts were rich in antioxidant constituents (Table 2). AWE exhibited higher total phenolic (322.9±34.69 µg GAE/mg) and flavonoid contents (318.5±74.14 µg QE/mg) compared to AEE (269.6±25.42 µg GAE/mg and 279.0±22.91 µg QE/mg, respectively), and the difference between the extracts was statistically significant ($p<0.05$). Despite this higher phenolic load, functional antioxidant assays indicated a tendency toward higher antioxidant activity for AEE in several assays (Fig. 2).

In the DPPH radical scavenging assay performed at a concentration of 30 µg/mL, AEE showed 95.53±2.72% inhibition, whereas AWE exhibited 79.60±9.17% inhibition, and this difference was statistically significant ($p<0.05$) (Table 3). Similarly, $ABTS^{\bullet+}$ scavenging activity was higher for AEE (97.20±1.05%) compared to AWE (73.50±2.20%), and the difference between the extracts was also statistically significant ($p<0.05$). When compared with standard antioxidants such as BHA, BHT, and α-tocopherol, the extracts exhibited comparable radical-scavenging capacities under the experimental conditions tested, rather than consistently exceeding these standards. Reducing power assays showed a similar pattern. AEE exhibited slightly higher Fe^{3+}, CUPRAC, and FRAP reducing capacities than AWE, although these differences were not statistically significant in all assays ($p>0.05$) (Table 4). Both extracts demonstrated measurable reducing activity, indicating their potential contribution to antioxidant capacity through electron-donating mechanisms. Although the DPPH, ABTS, FRAP, Fe^{3+} reducing, and CUPRAC assays are based on different reaction mechanisms, a similar activity trend was observed across the assays for the extracts. All antioxidant tests were conducted at the same extract concentration (30 µg/mL) under comparable experimental conditions, enabling direct comparison of the extracts. The consistent activity pattern observed across assays may therefore reflect the contribution of common redox-active phytochemicals present in the extracts rather than methodological similarities.

These results indicate that antioxidant efficacy may depend not only on total phenolic concentration but also on phenolic composition and the presence of specific bioactive constituents. According to the LC–MS/MS analysis, quinic acid and cyanidin-3-O-glucoside were identified as the predominant phenolic compounds in the extracts. Therefore, the observed antioxidant responses may be associated with the structural characteristics of these phenolics, particularly the presence of multiple hydroxyl groups that can donate hydrogen atoms and stabilize free radicals. Phenolic compounds such as quinic acid, anthocyanins (e.g., cyanidin-3-O-glucoside), and flavonoids detected in the extracts are known to exhibit notable redox properties due to their hydroxylated aromatic structures [64, 65]. Thus, the antioxidant activity observed in AEE may partly be attributed

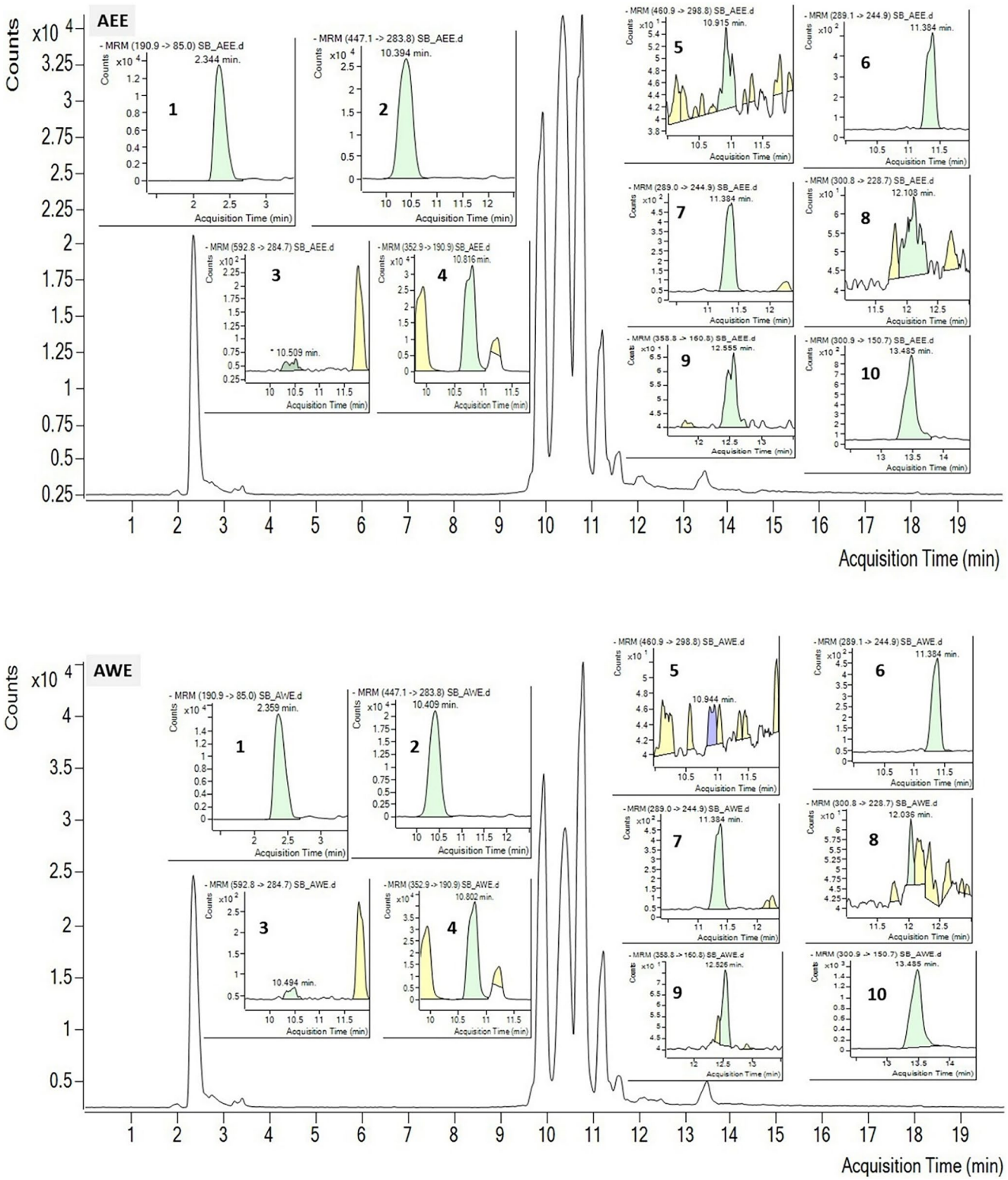

Fig. 1 LC–MS/MS chromatograms of aronia AEE and AWE Extracts: MRM resolutions of the metabolites

to the combined contribution of these phenolic constituents rather than to a single compound alone. Bioinformatic enrichment analyses further suggested that the predicted molecular targets of these compounds are associated with oxidative stress response and redox-regulated cellular pathways, which may support their potential antioxidant roles.

Table 2 Phytochemical analysis results of aronia extracts

Sample	Total phenolic content (µg GAE/mg)	Total flavonoid content (µg QE/mg)	Total reducing sugar content (µg ME/mg)
AEE	269.6 ± 25.42	279.0 ± 22.91	275.0 ± 6.46
AWE	322.9 ± 34.69	318.5 ± 74.14	274.0 ± 5.89

Antimicrobial activity

The antimicrobial activities of AWE and AEE extracts of *A. melanocarpa* were evaluated against selected Gram-positive and Gram-negative bacterial strains using disk diffusion and microdilution methods (Table 5). Both extracts exhibited antibacterial activity against all tested microorganisms; however, clear quantitative differences were observed between the two extraction solvents.

The ethanolic extract demonstrated consistently stronger antibacterial activity, with a MIC of 15.75 µg/mL against all tested strains, whereas the aqueous extract showed a higher MIC value of 31.25 µg/mL. Disk diffusion assays further supported this finding, as inhibition zone diameters produced by AEE were systematically larger than those observed for AWE, particularly against Gram-positive bacteria. This twofold difference in MIC values indicates a substantially higher antibacterial potency for the ethanolic extract.

The enhanced antimicrobial activity of AEE can be directly linked to its phenolic composition. As shown in the LC–MS/MS analysis, AEE contained a higher relative proportion of cyanidin-3-O-glucoside (40.61%) compared to AWE (27.42%), alongside notable levels of chlorogenic acid and minor flavonoids. Anthocyanins and phenolic acids are known to exert antibacterial effects through multiple mechanisms, including disruption of cell membrane integrity, increased membrane permeability, inhibition of

Table 3 Radical scavenging activities (%) of extracts and standard antioxidants against DPPH· and $ABTS^{+}$· radicals at a concentration of 30 µg/mL

Extracts / Standards	DPPH radical scavenging (%)	ABTS radical scavenging (%)
BHA	94.26 ± 1.53	91.40 ± 6.24
BHT	89.93 ± 1.53	88.40 ± 0.83
α-Tocopherol	84.60 ± 2.00	85.70 ± 5.82
AEE	95.53 ± 2.72	97.20 ± 1.05
AWE	79.60 ± 9.17	73.50 ± 2.20

*Values are expressed as mean ± SD (n=3). Differences between extracts and standard antioxidants were evaluated by ANOVA followed by Tukey's test. Differences were considered significant at $p < 0.05$

Table 4 FRAP, Fe3+, and Cu2+ reducing activities of extracts and standards at a concentration of 30 µg/mL

Extracts / Standards	Fe^{3+} reducing assay (λ700)	FRAP assay (λ595)	CUPRAC assay (λ450)
BHA[a]	2.394 ± 0.202	2.377 ± 0.136	2.338 ± 0.122
BHT[a]	2.280 ± 0.332	2.107 ± 0.229	1.941 ± 0.131
α-Tocopherol[a]	1.534 ± 0.165	1.711 ± 0.157	0.986 ± 0.086
AEE	2.289 ± 0.412	2.337 ± 0.117	2.453 ± 0.149
AWE	1.710 ± 0.174	1.755 ± 0.152	1.300 ± 0.136

Values are expressed as mean ± SD (n=3). Differences between extracts and standard antioxidants were evaluated by ANOVA followed by Tukey's test. Differences were considered significant at $p < 0.05$

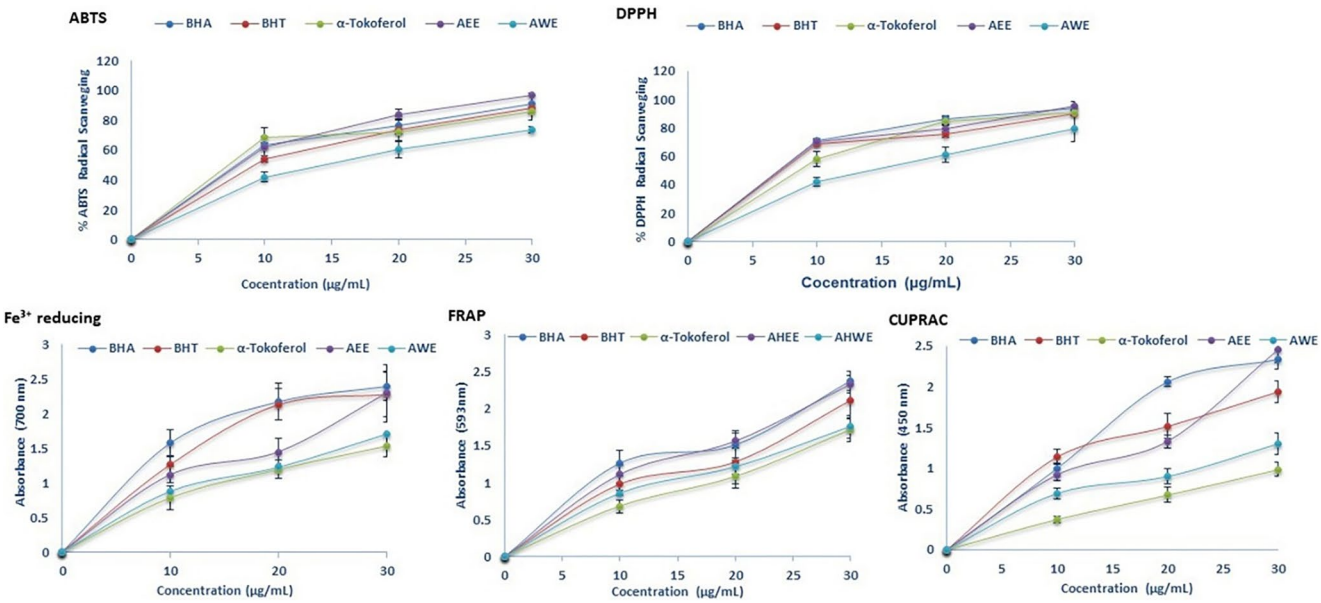

Fig. 2 A graphical representation of the antioxidant analysis results of aronia extracts ($p < 0.05$)

Table 5 MIC values and antimicrobial activities of plant extracts against selected bacterial strains

Bacteria	AEE (1000 µg/mL) Inhibition zone (mm)	AWE (1000 µg/mL) Inhibition zone (mm)	MIC (µg/mL) AEE	MIC (µg/mL) AWE	Negative control DMSO[b]	Positive control[c] (S) (mm)
Gram-positive bacteria						
B1	31.70 ± 0.85	33.43 ± 0.65	15.75	31.25	–	22.90 ± 5.06
B2	32.70 ± 0.75	30.26 ± 1.53	15.75	31.25	–	24.90 ± 2.86
Gram-negative bacteria						
B3	30.70 ± 0.85	28.93 ± 1.53	15.75	31.25	–	24.66 ± 4.39
B4	28.26 ± 2.52	30.00 ± 2.55	15.75	31.25	–	21.13 ± 2.10

Abbreviations: *B1Bacillus subtilis,B2Staphylococcus aureus,B3Escherichia coli,B4 Klebsiella pneumonia,GR+* GR positive, *GR−* GR negative, -, inhibition zone not formed

The inhibitory zone (mm) diameterfor different concentrations (µg mL^{-1})

Disc diameter: 5mm

[a]Extracts: Each at a concentration of 1000 µg/mL

[b]Negative Control: DMSO (10%)

[c]Positive Control: Antibacterial Standard Drug, S; Ampicillin (10 µg $disc^{-1}$) ($p < 0,05$)

Table 6 IC_{50} (µg/mL) values of Aronia extracts against metabolic enzymes

Samples	hCA I		hCA II		AChE		α-Glucosidase	
	IC_{50}	R^2	IC_{50}	R^2	IC_{50}	R^2	IC_{50}	R^2
AEE	38.50	0.9769	17.32	0.9766	11.55	0.9848	9.49	0.9856
AWE	46.20	0.9695	23.89	0.9814	18.72	0.9844	11.17	0.9827
Acetazolamide[1]	57.75	0.9779	40.76	0.9816	-	-	-	-
Tacrine[2]	-	-	-	-	21.65	0.9806	-	-
Acarbose[3]	-	-	-	-	-	-	30.13	0.9844

[1]Acetazolamide, [2]tacrine, and [3]acarbose were used as standards for hCA I-II, AChE, and α-glucosidase, respectively

bacterial enzymes, and interference with nucleic acid synthesis [66]. Although the present study did not experimentally investigate the precise antibacterial mechanism, the stronger activity observed for AEE may be associated with well-documented phenolic-mediated mechanisms, particularly membrane destabilization and enzyme inhibition, reported for anthocyanin-rich extracts. Therefore, the higher biological reactivity of the phenolic profile detected in AEE likely contributes to the observed antimicrobial efficacy [67, 68].

In agreement with previous studies, Gram-positive bacteria were generally more susceptible to both extracts than Gram-negative strains. This difference is commonly attributed to the presence of an outer lipopolysaccharide membrane in Gram-negative bacteria, which restricts the penetration of phenolic compounds [69]. Although the antibacterial activity of aronia extracts did not exceed that of conventional antibiotics, the relatively low MIC values, particularly for AEE, suggest that *A. melanocarpa* extracts may serve as effective complementary antimicrobial agents or natural preservatives, especially in food and nutraceutical contexts.

Enzyme Inhibition Results

The inhibitory effects of AWE and AEE against AChE, α-glycosidase, hCA I and II are summarized in Table 6. Both extracts exhibited strong inhibitory activity against all tested enzymes; however, the ethanolic extract consistently demonstrated superior potency, as reflected by lower IC50 values.

Specifically, AEE inhibited hCA I and hCA II with IC50 values of 38.50 µg/mL and 17.32 µg/mL, respectively, compared to 46.20 µg/mL and 23.89 µg/mL for AWE. Similarly, AEE showed stronger inhibition of AChE (IC50:11.55 µg/mL) than AWE (18.72 µg/mL). In the α-glycosidase inhibition assay, AEE again exhibited greater activity (IC50: 9.49 µg/mL) relative to AWE (11.17 µg/mL). Notably, both extracts demonstrated inhibitory effects that were stronger than those of the corresponding reference inhibitors used in the assays.

From a functional perspective, the inhibition of α-glycosidase is particularly relevant to postprandial glucose regulation and supports the antidiabetic potential of aronia

extracts. Likewise, AChE inhibition is directly associated with increased acetylcholine availability and is a key therapeutic strategy in neurodegenerative disorders. The observed inhibition of hCA I and II enzymes that play critical roles in ocular physiology and acid–base regulation represents a less explored but highly relevant aspect of aronia bioactivity.

The superior enzyme inhibitory performance of AEE mirrors its enhanced antioxidant and antimicrobial activities and can be attributed to its phenolic composition. Anthocyanins and flavonoids, particularly cyanidin-3-O-glucoside and quercetin derivatives, have been widely reported as effective inhibitors of AChE, α-glycosidase, and hCAs [69–72]. These findings indicate that *A. melanocarpa* extracts exert a multi-enzyme inhibitory profile, reinforcing the concept of a multi-target mode of action.

The relatively strong inhibitory activity observed for cyanidin-3-O-glucoside may be partially explained by structural features of the anthocyanin scaffold. In particular, the presence of a glycosyl group at the 3-position of the cyanidin backbone may influence the interaction of the molecule with the enzyme active site. Glycosylation can increase the number of hydrogen-bond donors and acceptors and may facilitate additional polar interactions with amino acid residues located in or near the catalytic pocket. Furthermore, the sugar moiety may affect the spatial orientation and conformational flexibility of the molecule, potentially stabilizing ligand–protein interactions within the binding cavity. These structural features may contribute to the comparatively stronger inhibitory activity observed for cyanidin-3-O-glucoside in the present study. Nevertheless, more detailed structure–activity relationship investigations involving additional anthocyanin derivatives would be required to fully elucidate the influence of glycosylation on enzyme inhibition.

Anticancer Activity

Cancer remains one of the leading causes of death worldwide, and the increasing mortality rates emphasize the urgent need for new preventive and therapeutic strategies [73]. Natural sources, particularly plants and microorganisms, have long been recognized as valuable reservoirs of bioactive compounds due to their chemical diversity, with more than 60% of current anticancer drugs being derived directly or indirectly from natural product [74]. Natural compounds can also be conjugated with conventional drugs or targeted delivery systems to enhance therapeutic efficacy and selectivity. This information highlights the potential of natural sources, particularly medicinal plants, as promising and safer alternatives for anticancer drug discovery [75]. In the present study, the cytotoxic activities of ethanol and water extracts of *A. melanocarpa*, which has the potential to provide new bioactive compounds and is rich in phenolic components, were evaluated on MCF-7 and A549 cells using the CVDK-8 test. For this purpose, cells were exposed to extracts at concentrations ranging from 0 to 1000 µg/mL for 48 h. As demonstrated in Fig. 3A, neither extract exhibited a substantial cytotoxic effect in MCF-7 cells, despite the presence of elevated concentrations. Conversely, in A549 cells, both AEE- and AWE-treated groups exhibited significant morphological alterations, including cell shrinkage and rounding, in comparison to the control group (Fig. 3B). Furthermore, the cytotoxic effect of AEE was observed to be more pronounced than that of AWE in A549 cells, and the IC50 value for AEE was calculated as 943.21 ± 7.25 µg/mL after 48 h of incubation. These findings are consistent with literature reports showing that the cytotoxic activity of Aronia extracts varies depending on the cell line and extraction method. For instance, the purified phenolic-rich extract (APE) showed significant cytotoxicity in the SW-480 colon cancer cell line (IC50 value: 194.35 µg/mL) after 48 h. In HT-29 cells, APE exhibited stronger cytotoxicity with an IC50 value of 552.02 µg/mL, compared to 794.84 µg/mL for the phenolic-rich aronia extract (ACE). The IC50 values at 72 h in normal intestinal epithelial cells (CCD 841 CoN) were reported as 594 µg/mL for APE and 709 µg/mL for ACE. These data demonstrate that the extracts can exhibit selective cytotoxic effects on cancer cells, showing a particularly strong anticancer potential in SW-480 cells [76]. Another study reported that Aronia extracts exhibited moderate cytotoxic effects on MCF-7 and HeLa cell lines, with ethanol extracts showing the strongest activity [77]. These results indicate that the cytotoxic activity of *A. melanocarpa* extracts depends on both the solvent and the cell type. The fact that *A. melanocarpa* extracts exhibit cytotoxic effects in A549 cells but not in MCF-7 cells suggests a cell type-dependent response. This difference may be related to variations in cellular metabolism or sensitivity to cell death. Overall, these findings suggest that *A. melanocarpa* extracts may be a potential source of bioactive compounds. However, further mechanistic and *in vivo* studies are needed to confirm and better understand these effects.

In Silico Studies

While quinic acid is quantitatively the dominant compound in the extracts, the correlation between abundance and biological activity is not always linear. To elucidate the molecular mechanism responsible for the observed enzyme inhibition, induced-fit molecular docking studies were conducted for the three most abundant compounds: quinic acid, cyanidin-3-O-glucoside, and chlorogenic acid. The docking results revealed a compelling discrepancy between compound abundance and binding affinity. As shown in Table 7,

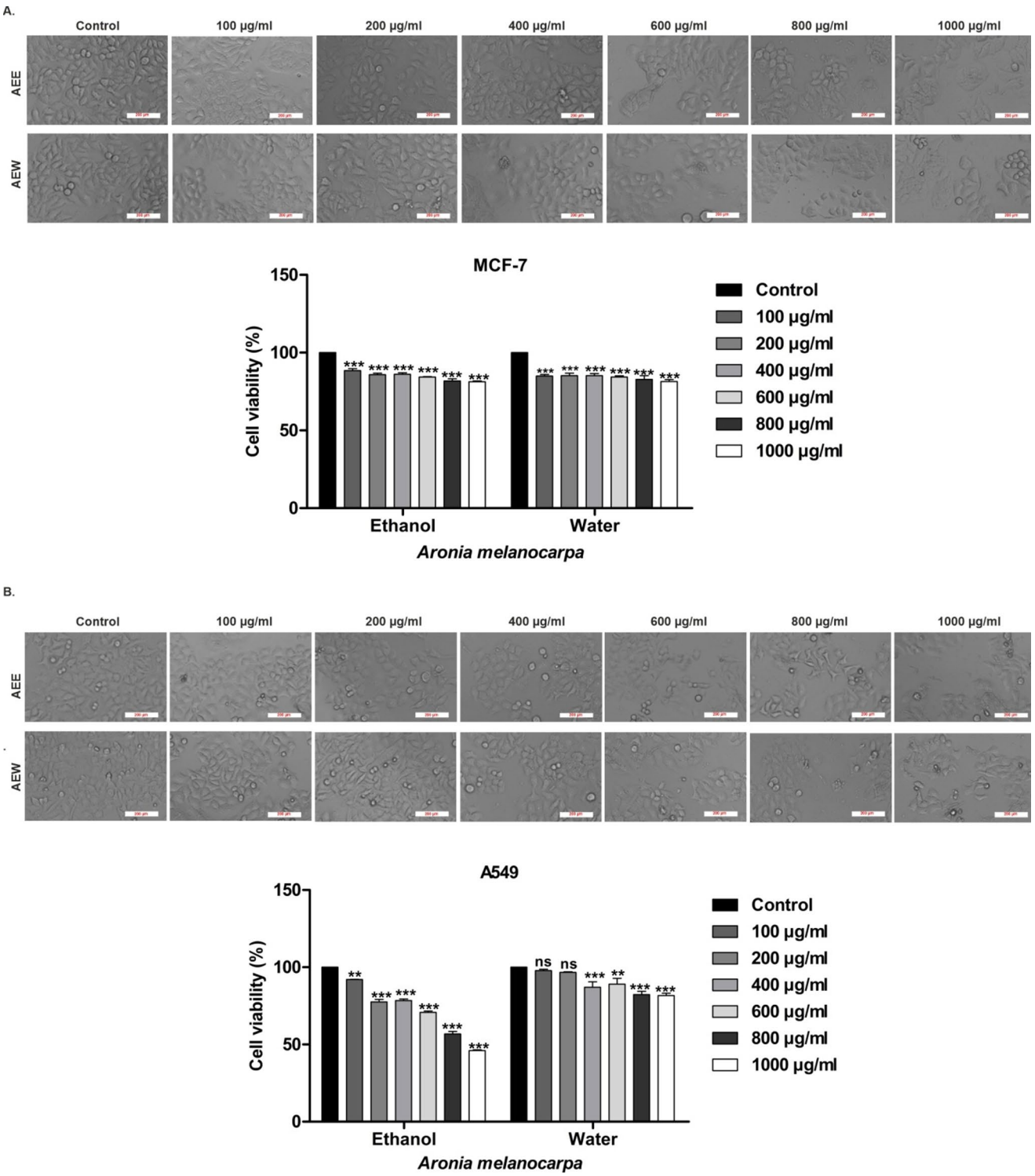

Fig. 3 Effects of AEE and AWE on the viability of MCF-7 and A549 cells. Inverted microscope images and CVDK-8 viability analysis of MCF-7 (**A**) and A549 (**B**) cells treated with different concentrations (0–1000 µg/mL) of AEE and AWE for 48 h. $^{**}p<0.01$, and $^{***}p<0.001$ in relation to the control. Scale bar, 200 µm

cyanidin-3-O-glucoside consistently exhibited significantly higher binding scores (indicating stronger affinity) across all tested enzymes compared to the more abundant quinic acid.

The most striking difference was observed in AChE inhibition. Cyanidin-3-O-glucoside achieved a docking score of -23.960 kcal/mol, which is vastly superior to quinic acid

Table 7 Induced-fit molecular docking scores of the three most abundant compounds in aronia plant extracts against the relevant enzymes

Compounds	hCA IIFD Docking Score(kcal/mol)	hCA IIIFD Docking Score(kcal/mol)	AChEIFD Docking Score(kcal/mol)	α-glucosidaseIFD Docking Score(kcal/mol)
Cyanidin-3-O-glucoside	-12.025	-13.267	-23.960	-13.138
Chlorogenic acid	-12.843	-12.057	-12.527	-10.514
Quinic acid	-9.515	-10.049	-7.739	-6.455
Tacrine	-	-	-13.857	-
Acetazolamide	-7.794	-8.386	-	-
Acarbose	-	-	-	-10.453

(-7.739 kcal/mol) and even surpasses the standard inhibitor tacrine (-13.857 kcal/mol). This suggests that despite being the second most abundant compound, cyanidin-3-O-glucoside is likely the primary contributor to the potent AChE inhibition observed in the in vitro assays. The docking pose of cyanidin-3-O-glucoside within the AChE active site reveals a complex network of interactions. The ligand forms critical hydrogen bonds with amino acid residues TRP84, GLY117, GLY118, TYR130 SER200, GLH199, and ASP72. Furthermore, strong Pi-Pi stacking interactions are observed between the aromatic rings of the cyanidin scaffold and residues TRP84 and PHE330, along with Pi-cation interactions at the oxonium core (Fig. 4A). These hydrophobic and electrostatic interactions likely stabilize the bulky glycoside structure within the enzyme's gorge, explaining the exceptionally high docking score of -23.960 kcal/mol.

A similar trend was observed for hCA I, hCA II, and alpha-glycosidase, where cyanidin-3-O-glucoside displayed scores of -12.025, -13.267, and -13.138 kcal/mol, respectively, consistently outperforming quinic acid. In the case of hCA II, cyanidin-3-O-glucoside fits securely into the active site, anchored by hydrogen bonds with ASN62, ASN67, GLN92, THR199, and THR200. It establishes a metal coordination interaction with the catalytic zinc ion (ZN302) in the hCA II active site (Fig. 4B). Similar hydrogen bonding networks involving GLN92 and THR199 were observed for hCA I. Cyanidin-3-O-glucoside also double hydrogen binding with HIS122 in the active site of hCAI. It establishes a metal coordination interaction with the catalytic zinc ion (ZN301) in the hCAI active site (Fig. 4C). These specific polar interactions mimic the binding mode of sulfonamide-based inhibitors, thereby blocking the catalytic center.

In the α-glucosidase active site, cyanidin-3-O-glucoside establishes an extensive hydrogen-bonding network with catalytic residues such as ASP203, ASH327, ASH366, TRP406, ASP443, HIE600, TYR605, and GLN603, contributing significantly to the stabilization of the enzyme–ligand complex (Fig. 4D).

The ADME properties of the major compounds identified in *A. melanocarpa* extracts quinic acid, chlorogenic acid, and cyanidin-3-O-glucoside were evaluated using QikProp predictions (Table 8). The calculated molecular weights ranged from 192.168 to 448.382 Da, with quinic acid exhibiting the lowest value and cyanidin-3-O-glucoside the highest. Hydrogen-bond donor and acceptor counts varied between 5–7 and 7.85–14.0, respectively, indicating a relatively high polarity for all compounds. Consistently, the predicted lipophilicity (QPlogPo/w) values were negative (− 1.234 to − 0.228), suggesting limited hydrophobic character. The predicted aqueous solubility (QPlogS) values ranged from − 1.012 to − 2.640, indicating moderate solubility across the compounds. Regarding cardiotoxicity risk, QPlogHERG values varied from − 0.799 to − 5.333, with cyanidin-3-O-glucoside showing the lowest value. Predicted intestinal permeability values (QPPCaco) were relatively low, ranging from 1.725 to 11.084 nm/s, while MDCK cell permeability (QPPMDCK) values ranged between 0.649 and 4.845 nm/s, suggesting limited membrane permeability. Similarly, the predicted brain/blood partition coefficients (QPlogBB) were strongly negative (− 1.637 to − 3.313), indicating poor blood–brain barrier penetration. The predicted human oral absorption values were modest, ranging from 10.35% to 38.42%, with quinic acid showing the highest absorption. Evaluation of drug-likeness rules revealed that quinic acid did not violate Lipinski's rule of five, whereas chlorogenic acid and cyanidin-3-O-glucoside showed one and two violations, respectively. A similar pattern was observed for the rule of three, where quinic acid and chlorogenic acid exhibited one violation and cyanidin-3-O-glucoside two violations (Table 8). Overall, these results indicate that the investigated phenolic constituents possess relatively polar physicochemical characteristics with moderate solubility but limited predicted membrane permeability and oral absorption. Nevertheless, the obtained ADME profiles provide valuable insight into the pharmacokinetic limitations of these natural compounds and may serve as a useful framework for guiding future structural optimization studies or the design and discovery of novel derivatives with improved drug-like properties [20, 25].

Aronia extracts, molecular docking simulations strongly suggest that cyanidin-3-O-glucoside is the principal agent responsible for the observed enzymatic inhibition. The superior docking scores of cyanidin-3-O-glucoside, particularly against AChE (-23.960), indicate that its structural features allow for more favorable energetic interactions with the enzymes' active sites compared to quinic acid. Therefore, the therapeutic potential of Aronia extracts appears to

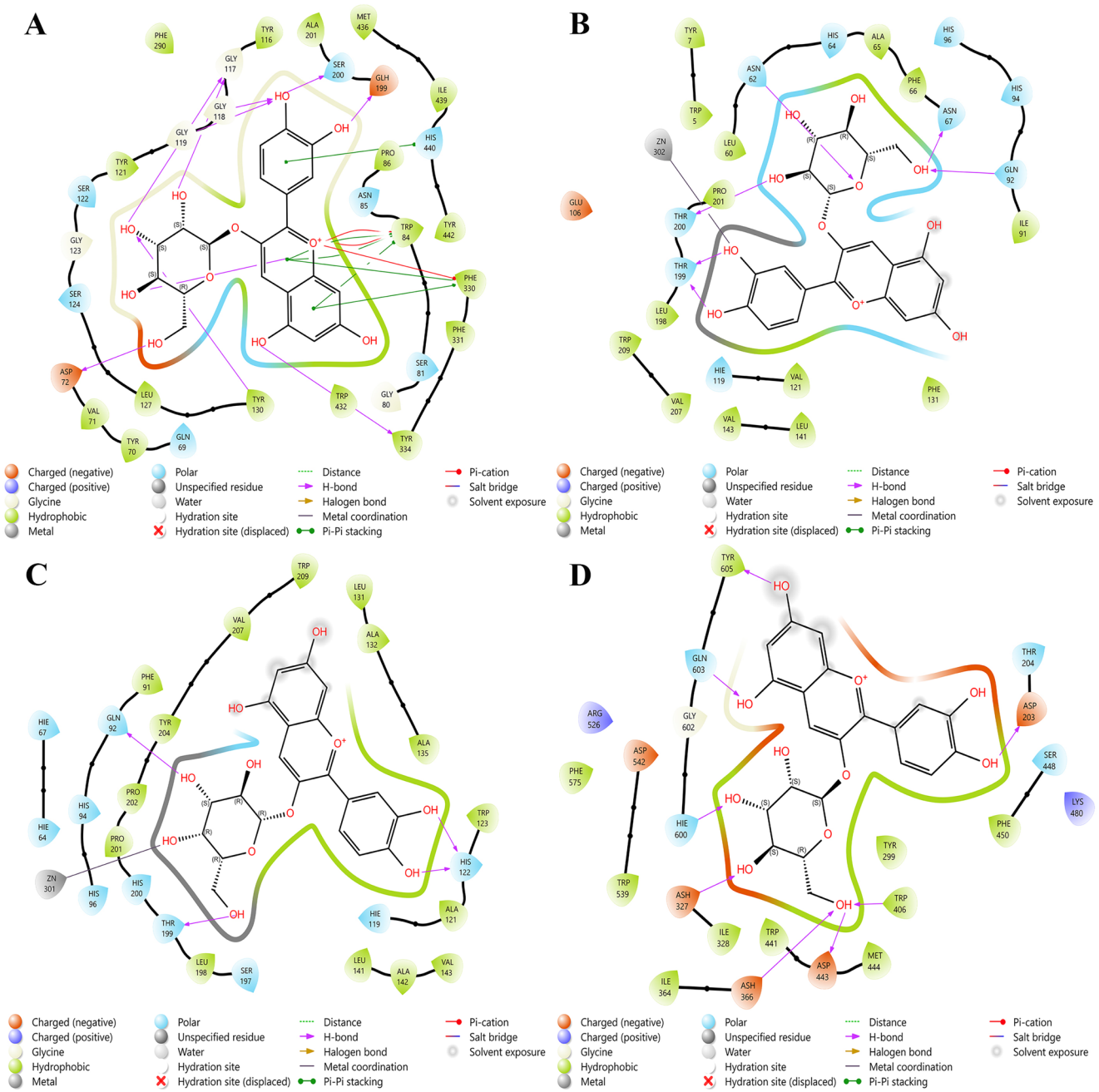

Fig. 4 Two-dimensional interaction diagrams depicting the binding modes of the ligand cyanidin-3-O-glucoside within the active sites of the respective target protein complexes: (**A**) AChE (PDB ID: 4TVK), (**B**) hCA I (PDB ID: 4WR7), (**C**) hCA II (PDB ID: 8J2O), and (**D**) α-glucosidase (PDB ID: 2QMJ)

be driven by the high affinity of anthocyanins like cyanidin-3-O-glucoside, rather than the sheer quantity of organic acids.

It is increasingly recognized that individual phytochemicals can exert pleiotropic biological activities by interacting with multiple molecular targets and signaling pathways. In this context, several plant-derived compounds have been described as multifunctional bioactive molecules capable of modulating diverse biological processes such as oxidative stress regulation, inflammation, and cancer-related signaling pathways. For example, drimenol has recently been characterized as a phytochemical with broad-spectrum bioactivities, including antioxidant, anti-inflammatory, and anticancer effects mediated through interactions with multiple cellular targets [78]. This concept supports the present findings, where cyanidin-3-O-glucoside despite not being the most abundant compound in the extract exhibited the strongest docking interactions with several enzyme targets.

Table 8 Predicted ADME properties of the compounds identified in *A. melanocarpa* extracts calculated using the QikProp module in Maestro 13.9

Compound	mol MW	donorHB	acceptHB	QPlogPo/w	QPlogS	QPlogHERG	QPPCaco	QPlogBB	QPPMDCK	%HOA	Rule Of Five	Rule Of Three
Quinic acid	192.168	5.000	7.850	-1.234	-1.012	-0.799	11.084	-1.637	4.845	38.419	0	1
Chlorogenic acid	354.313	6.000	9.650	-0.228	-2.526	-3.277	1.725	-3.313	0.649	16.891	1	1
Cyanidin-3-O-glucoside	448.382	7.000	14.000	-1.173	-2.640	-5.333	8.029	-3.198	2.689	10.350	2	2

*MW: molecular weight (130–725); donorHB: hydrogen-bond donors (0–6); acceptHB: hydrogen-bond acceptors (2–20); QPlogPo/w: predicted octanol/water partition coefficient (−2.0 to 6.5); QPlogS: predicted aqueous solubility (−6.5 to 0.5); QPlogHERG: predicted IC_{50} value for blockage of the HERG K^+ channel (values below −5 indicate potential risk of cardiotoxicity); QPlogBB: predicted brain/blood partition coefficient (−3.0 to 1.2); QPPCaco: predicted Caco-2 cell permeability (<25 poor, >500 great); QPPMDCK: predicted MDCK cell permeability (<25 poor, >500 great); QPlogHERG: predicted HERG channel inhibition (concern when < −5); %HOA: predicted human oral absorption (0–100%; <25 low, >80 high). Rule of Five and Rule of Three represent the number of violations of Lipinski's rule of five and Jorgensen's rule of three, respectively, which are commonly used criteria for evaluating drug-likeness. The recommended ranges correspond to the values typically observed for approximately 95% of known drugs

Therefore, similar to other multifunctional phytochemicals, cyanidin-3-O-glucoside may act as a key bioactive driver of the diverse biological effects observed for *A. melanocarpa* extracts.

Bioinformatic and Functional Enrichment Results

The functional enrichment and disease association studies were carried out to explain the biological activities of the common target genes of quinic acid, chlorogenic acid, and cyanidin 3-O-glucoside that predicted potential molecular pathways. The enrichment findings were consistently directed to the pathway and biological processes that are related to the regulation of oxidative stress, inflammatory reactions, metabolic regulation, and cell survival mechanisms.

Disease Association Analysis (DisGeNET)

The DisGeNET database revealed that the predicted targets of the major phenolic compounds were significantly associated with several metabolic and pathological conditions. The most significantly enriched disease categories included hyperlipidemia, dyslipidemias, and hypercholesterolemia, suggesting a strong connection between the identified targets and lipid metabolism disorders. In addition, disease terms such as reperfusion injury, brain ischemia, and mechanical allodynia were also enriched, indicating potential involvement of these targets in oxidative stress- and inflammation-related pathological processes. Notably, several cancer-related disease terms, including fibroid tumor, hepatoblastoma, and childhood solid neoplasm, were also identified, suggesting that the phenolic constituents of Aronia melanocarpa may influence molecular pathways associated with tumor development and cellular proliferation. Collectively, these findings highlight the potential therapeutic relevance of the identified phenolic compounds in metabolic, inflammatory, and cancer-related disorders (Fig. 5A).

GO-BP Enrichment

GO biological process enrichment analysis revealed that the predicted targets of the major phenolic compounds were significantly associated with several cellular regulatory and metabolic processes. Among the most significantly enriched terms were positive regulation of MAPK cascade, positive regulation of phosphorus and phosphate metabolic processes, and regulation of protein transport, indicating a strong involvement of phosphorylation-related signaling networks. In addition, pathways related to organic acid transport, carboxylic acid transport, and fatty acid transport were also enriched, suggesting a potential role of

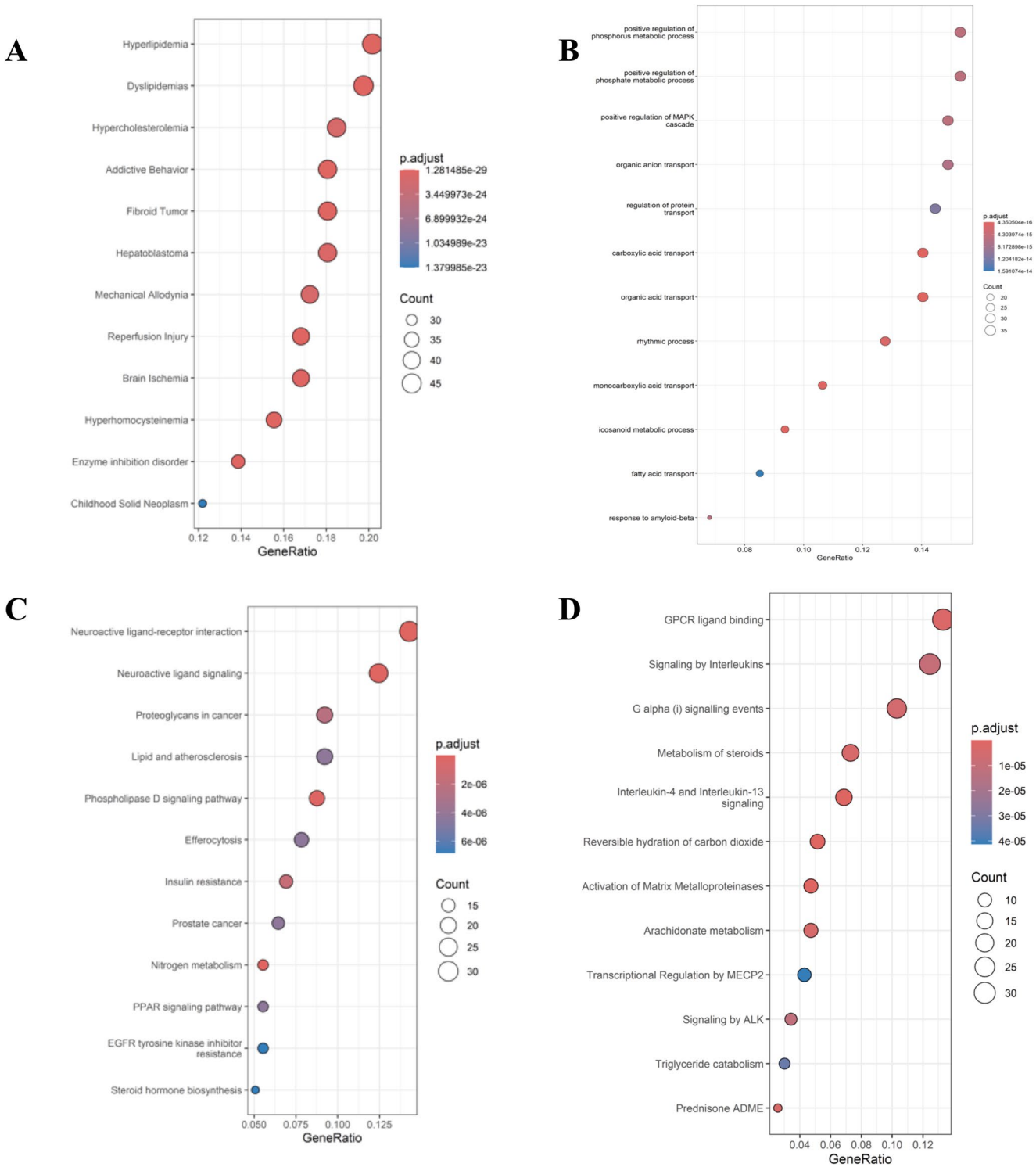

Fig. 5 Bioinformatic enrichment analysis of molecular targets associated with the major phenolic compounds (quinic acid, cyanidin-3-O-glucoside, and chlorogenic acid) of *A. melanocarpa*. (**A**) Disease association analysis based on the DisGeNET database, (**B**) GO Biological Process (**C**) KEGG pathway enrichment analysis, (**D**) Reactome pathway enrichment analysis

these compounds in the modulation of cellular metabolic fluxes and membrane transport systems. Notably, processes linked to icosanoid metabolic process and response to amyloid-beta were also identified, which are often associated with inflammatory and oxidative stress-related cellular responses. Overall, these findings suggest that the phenolic constituents of Aronia melanocarpa may exert their biological activities through the coordinated regulation of signaling pathways, metabolic processes, and stress-responsive mechanisms. (Fig. 5B).

KEGG Pathway Enrichment Analysis

KEGG pathway enrichment analysis revealed that the predicted targets of the major phenolic compounds were significantly associated with several signaling and disease-related pathways. Among the most enriched pathways were neuroactive ligand–receptor interaction and neuroactive ligand signaling, indicating the potential involvement of receptor-mediated signaling mechanisms. In addition, pathways related to proteoglycans in cancer, phospholipase D signaling pathway, and EGFR tyrosine kinase inhibitor resistance were also significantly enriched, suggesting a potential role of these compounds in modulating cancer-associated signaling networks and cellular proliferation pathways. Metabolic and inflammation-related pathways such as lipid and atherosclerosis, nitrogen metabolism, and PPAR signaling pathway were also identified, highlighting the possible involvement of these phenolic compounds in lipid metabolism and metabolic regulation. Furthermore, enrichment of pathways such as insulin resistance and steroid hormone biosynthesis suggests broader regulatory effects on endocrine and metabolic processes. This further increases the number of cancer-associated KEGG pathways which supports the cytotoxic nature of the A549 cell which further serves to suggest that the proposed targets can help regulate cell survival and proliferation pathways. All these findings suggest that the possible action of the compounded effects of the *A. melanocarpa* compounds is through a set of interconnected metabolic and signaling networks, as opposed to a single molecular target (Fig. 5C). Based on these findings, oxidative stress–related signaling and apoptosis pathways were considered the most plausible mechanisms underlying the selective cytotoxicity observed in A549 cells.

Reactome Pathway Analysis

Reactome pathway enrichment analysis further revealed that the predicted targets of the major phenolic compounds were significantly involved in several receptor-mediated signaling and inflammatory pathways. Among the most significantly enriched pathways were GPCR ligand binding, signaling by interleukins, and G alpha (i) signaling events, indicating that the identified targets are closely associated with receptor-driven signal transduction and immune-related cellular responses. In addition, pathways such as interleukin-4 and interleukin-13 signaling and activation of matrix metalloproteinases suggest potential involvement in inflammatory regulation and extracellular matrix remodeling (Fig. 5D). Metabolic pathways, including metabolism of steroids, arachidonate metabolism, and triglyceride catabolism, were also enriched, highlighting possible roles in lipid metabolism and metabolic homeostasis. Collectively, these findings indicate that the phenolic constituents of *A. melanocarpa* may exert their biological activities through the modulation of multiple signaling networks associated with immune regulation, receptor-mediated signaling, and metabolic processes.

Although the present findings demonstrate promising biological activities of *A. melanocarpa* extracts, the therapeutic application of phenolic compounds may be constrained by their relatively low stability, limited intestinal absorption, and rapid metabolic transformation. Such pharmacokinetic limitations are widely recognized for many polyphenolic compounds, including anthocyanins and phenolic acids. In recent years, nanotechnology-based formulation strategies have emerged as effective approaches to enhance the bioavailability and pharmacological performance of natural bioactives. In particular, nanoparticle-based delivery systems and nanoencapsulation technologies have been extensively investigated to improve compound stability, enable controlled release, and enhance cellular uptake. For instance, calcium carbonate nanoparticle ($CaCO_3$-NP) platforms have been shown to significantly enhance the delivery and therapeutic efficacy of antioxidant compounds such as thymoquinone when combined with conventional anticancer agents [79, 80]. Moreover, recent studies highlight that $CaCO_3$ nanocarriers can provide controlled drug release and tumor-targeted delivery, thereby improving therapeutic selectivity and safety profiles [81]. In this context, similar nano-delivery strategies could potentially enhance the stability, bioavailability, and therapeutic performance of the major phenolic constituents of *A. melanocarpa*, particularly cyanidin-3-O-glucoside and chlorogenic acid.

Conclusion

The present paper is an in-depth analysis of the biological potential of the extracts of the Aronia melanocarvae by combining quantitative phytochemical profiling, *in vitro* bioactivity determination, molecular docking, and bioinformatic enrichment studies. The results obtained by LC–MS/MS showed that aqueous and ethanolic extracts both

contain high concentrations of phenolic compounds, with the most significant ones being quinic acid, cyanidin-3-O-glucoside, and chlorogenic acid. The aqueous extract had higher total phenolic and flavonoid total content, the ethanolic extract continued to have high functional performance in antioxidant, antimicrobial and enzyme inhibition assays, which demonstrates the significance of phenolic composition, not the total phenolic content. The ethanolic extract was functionally characterized by high radical-scavenging potential, decreased MIC values with respect to bacterial strains tested and potent inhibition of alpha-glycosidase, acetylcholinesterase, and human carbonic anhydrase isoenzymes in some cases being superior to standard reference inhibitors. Moreover, the extracts showed cytotoxic activity in A549 lung cancer cells, while exhibiting limited effects on MCF-7 breast cancer cells, indicating potential cell type-specific activity. These results were further confirmed using molecular docking in which cyanidin-3-O-glucoside was identified as having high-affinity binding to various enzyme targets, although it is not the most abundant one. Lastly, bioinformatics enrichment studies revealed that the common targets of the major phenolic compounds are linked to oxidative stress response, metabolic regulation, inflammation and cell survival pathways, which provided a network-level perspective of the bioactivities observed. In aggregate, these findings suggest that the effects of the extracts of the species, *A. melanocarpa* are multi-target and systems-based. The results indicate the possible potential of using the *A. melanocarpa* and especially its ethanolic extract as a promising source of multifunctional bioactive substances in food, nutraceutical, and pharmacological perspectives in the future besides serving as a mechanistic framework to support future targeted *in viv*o and clinical studies. However, the physiological relevance of these findings may depend on the bioavailability and metabolic stability of phenolic compounds such as cyanidin-3-O-glucoside. The strong antioxidant, antimicrobial, and enzyme inhibitory activities observed in this study suggest that aronia extracts may have potential applications as natural food preservatives and as functional ingredients in nutraceutical formulations.

Supplementary Information The online version contains supplementary material available at https://doi.org/10.1007/s11483-026-10129-5.

Author contributions Cansu Öztürk: writing–original draft, writing–review and editing, project administration, conceptualization, validation, investigation, data curation. Songül Bayrak: writing–original draft, writing–review and editing, project administration, conceptualization, validation, investigation, data curation. Şeyda Nur Kalın: visualization, formal analysis, validation, conceptualization, writing–review and editing. Namık Kılınç: visualization, formal analysis, validation, conceptualization, writing–review and editing. Yeliz Demir: visualization, formal analysis, validation, conceptualization, writing–original draft, writing–review and editing. Ö. İrfan Küfrevioğlu: data curation, validation, conceptualization.

Funding Open access funding provided by the Scientific and Technological Research Council of Türkiye (TÜBİTAK). This study did not receive any support.

Data Availability No datasets were generated or analysed during the current study.

Declarations

Generative AI statement Our research team utilized AI-assisted tools solely for language enhancement and readability improvement during the manuscript preparation process.

Competing interests The authors declare no competing interests.

Open Access This article is licensed under a Creative Commons Attribution 4.0 International License, which permits use, sharing, adaptation, distribution and reproduction in any medium or format, as long as you give appropriate credit to the original author(s) and the source, provide a link to the Creative Commons licence, and indicate if changes were made. The images or other third party material in this article are included in the article's Creative Commons licence, unless indicated otherwise in a credit line to the material. If material is not included in the article's Creative Commons licence and your intended use is not permitted by statutory regulation or exceeds the permitted use, you will need to obtain permission directly from the copyright holder. To view a copy of this licence, visit http://creativecommons.org/licenses/by/4.0/.

References

1. K. Özdemir, Y. Demir, Food Sci. Nutr. **13**, e70714 (2025)
2. C. Wan, S. Langyan, J. Echeverría, H.P. Devkota, D. Tewari, M.A. Moosavi, S.M. Ezzat, A. Perez-Vazquez, M. Fraga-Corral, G. Cravotto, M.A. Prieto, T. Belwal, M. Li, Phytochem Rev. **24**, 1197–1225 (2025)
3. S. Sergazy, Z. Shulgau, Y. Kamyshanskiy, Z. Zhumadilov, E. Krivyh, A. Gulyayev, M. Aljofan, Heliyon 9 Heliyon. **9**(4), e15370 (2023)
4. H. Jung, H.K. Kwak, K.T. Hwang, Food Sci. Biotechnol. **23**, 2053–2062 (2014)
5. H.P. Amin, C. Czank, S. Raheem, Q. Zhang, N.P. Botting, A. Cassidy, C.D. Kay, Mol. Nutr. Food Res. **59**, 1095–1106 (2015)
6. S.K. Panchal, L. Brown, Molecules. **28**, 80 (2022)
7. P.S. Mistry, M.R. Chorawala, B.S. Sivamaruthi, B.G. Prajapati, A. Kumar, C. Chaiyasut, Curr. Diabetes Rev. **21**, e15733998322754 (2025)
8. M. Saracila, A.E. Untea, A.G. Oancea, I. Varzaru, P.A. Vlaicu, Foods. **13**, 1856 (2024)
9. L. Jakobek, M. Šeruga, M. Medvidović-Kosanović, I. Novak, Agric. Conspec Sci. **72**, 301–306 (2007)
10. A. Kokotkiewicz, Z. Jaremicz, M. Luczkiewicz, J. Med. Food. **13**, 255–269 (2010)
11. A. Sidor, A. Drożdżyńska, A. Gramza-Michałowska, Trends Food Sci. Technol. **89**, 45–60 (2019)
12. T. Jurendić, M. Ščetar, Antioxidants. **10**, 1052 (2021)
13. E.Y. Platonova, M.V. Shaposhnikov, H.Y. Lee, J.H. Lee, K.J. Min, A. Moskalev, Trends Food Sci. Technol. **114**, 570–584 (2021)
14. Z. Yang, X. Deng, Z. Yang, M. Han, N. Ismail, K.W. Chan, M.Z.A. Bakar, Food Biosci. **60**, 104511 (2024)
15. Y. Zhang, Y. Zhao, X. Liu, X. Chen, C. Ding, L. Dong, J. Zhang, S. Sun, Q. Ding, S. Khatoom, Z. Cheng, W. Liu, L. Shen, F. Xiao, J. Future Foods. **1**, 168–178 (2021)
16. O. Frumuzachi, A. Mocan, S. Rohn, L. Gavrilaş, Nutrients. **17**, 1488 (2025)

17. D. Shi, J. Xu, L. Sheng, K. Song, Molecules. **29**, 1388 (2024)
18. J. Xu, F. Li, M. Zheng, L. Sheng, D. Shi, K. Song, Plants. **13**, 3557 (2024)
19. S.M. Paunović, P. Mašković, M. Milinković, Erwerbs-Obstbau. **64**, 581–589 (2022)
20. Z. Yang, Z. Yang, M.Z.A. Bakar, X. Deng, Microchem J. **210**, 112917 (2025)
21. B. Kuzu, Y. Demir, Arch. Biochem. Biophys. **771**, 110504 (2025)
22. F.S. Tokalı, Y. Demir, Ş. Ateşoğlu, P. Tokalı, H. Şenol, Arch. Pharm. **358**, e70033 (2025)
23. Z. Bulut, N. Abul, A. Halıç Poslu, İ. Gülçin, A. Ece, E. Erçağ, Ö. Koz, G. Koz, J. Mol. Struct. **1280**, 135047 (2023)
24. V. Tahiroglu, H. Karagecili, K. Aslan, İ. Gulcin, Life. **15**, 1209 (2025)
25. Z. Yang, C.L. Cespedes-Acuna, Z. Yang, M.Z. Abu Bakar, K.W. Chan, X. Deng, Food Rev. Int. **41**, 1390–1439 (2025)
26. K. Aslan, K. Kelle, M.A. Yilmaz, E. Erden Kopar, I. Gulcin, ChemistrySelect 9, e202403588 (2024)
27. N. Balci, K. Aslan, A. Erturk, I. Gulcin, Food Sci. Nutr. **13**, e70654 (2025)
28. P.N. Denev, C.G. Kratchanov, M. Ciz, A. Lojek, M.G. Kratchanova, Compr. Rev. Food Sci. Food Saf. **11**, 471–489 (2012)
29. A. Sidor, A. Gramza-Michałowska, Molecules. **24**, 3710 (2019)
30. M. Isıyel, H. Ceylan, Y. Demir, Biol. Trace Elem. Res. **204**, 1068–1083 (2026)
31. A.Z. Tel, K. Aslan, M.A. Yılmaz, İ. Gulcin, Food Chem. X. **25**, 102125 (2025)
32. Z. Bingöl, Biotechnol. Appl. Biochem. **72**, 924–935 (2025)
33. İ. Gulcin, R. Kaya, A.C. Goren, H. Akincioglu, M. Topal, Z. Bingol, K. Cetin, S.B. Çakmak, L. Ozturk Sarikaya, S. Durmaz, Alwasel, Int. J. Food Prop. **22**, 1511–1526 (2019)
34. B. Okutucu, S. Önal, Talanta. **87**, 74–79 (2011)
35. H. Can, L. Güven, F.D. Miloğlu, Abd El-Aty. Microchem J. **201**, 110683 (2024)
36. L. Güven, H. Can, A. Ertürk, F.D. Miloğlu, M. Koca, F. İnce, İ. Gülçin, S Afr. J. Bot. **165**, 478–493 (2024)
37. M.S. Blois, Nature. **181**, 1199–1200 (1958)
38. M. Oyaizu, Jpn J. Nutr. Diet. **44**, 307–315 (1986)
39. R. Apak, K. Güçlü, M. Özyürek, S.E. Karademir, J. Agric. Food Chem. **52**, 7970–7981 (2004)
40. S. Bayrak, S. Gerni, C. Öztürk, Z. Almaz, Ç. Bayrak, N. Kılınç, H. Özdemir, J. Biochem. Mol. Toxicol. **38**, e70055 (2024)
41. D. Ruzgar, Y. Akbaba, B. Ozgeris, A. Gormez, Nat. Prod. Biotechnol. **2**, 81–87 (2022)
42. G.L. Ellman, K.D. Courtney, V. Jr. Andres, R.M. Featherstone, Biochem. Pharmacol. **7**, 88–95 (1961)
43. C. Öztürk, E. Kalay, S. Gerni, N. Balci, F.S. Tokali, O.N. Aslan, E. Polat, Biotechnol. Appl. Biochem. **71**, 223–231 (2024)
44. J.A. Verpoorte, S. Mehta, J.T. Edsall, J. Biol. Chem. **242**, 4221–4229 (1967)
45. Y. Tao, Y. Zhang, Y. Cheng, Y. Wang, Biomed. Chromatogr. **27**, 148–155 (2013)
46. Ş.N. Kalın, A. Altay, H. Budak, Life Sci. **310**, 121093 (2022)
47. Ş. Günaydın, Ş.N. Kalın, E.K. Sulukoğlu, A. Altay, H. Budak, Naunyn-Schmiedebergs Arch. Pharmacol. **398**, 17445–17458 (2025)
48. W. Sherman, T. Day, M.P. Jacobson, R.A. Friesner, R. Farid, J. Med. Chem. **49**, 534–553 (2006)
49. A. Akıncıoğlu, S. Göksu, A. Naderi, H. Akıncıoğlu, N. Kılınç, İ. Gülçin, Comput. Biol. Chem. **94**, 107565 (2021)
50. N. Gök, A. Akıncıoğlu, E. Erümit Binici, H. Akıncıoğlu, N. Kılınç, S. Göksu, Arch. Pharm. **354**, 2000496 (2021)
51. Z. Alım, H. Şirinzade, N. Kılınç, E. Dilek, S. Süzen, J. Mol. Struct. **1311**, 138276 (2024)
52. S. Dawbaa, C. Türkeş, D. Nuha, Y. Demir, A.E. Evren, L. Yurttaş, Ş. Beydemir, J. Biomol. Struct. Dyn. **43**, 9599–9617 (2025)
53. C. Efeoglu, Y. Demir, C. Türkeş, E. Yabalak, Z. Seferoglu, Y. Nural, Arch. Biochem. Biophys. **130**, 110515 (2025)
54. F.S. Tokalı, H. Şenol, Ş. Ateşoğlu, P. Tokalı, F. Akbaş, J. Mol. Struct. **1319**, 139519 (2025)
55. R. Sağlamtaş, Y. Demir, S. Küçük, F. Özgökçe, V. Çomakli, Eur. Food Res. Technol. **251**, 4719–4736 (2025)
56. T. Jurikova, J. Mlcek, S. Skrovankova, D. Sumczynski, J. Sochor, I. Hlavacova, L. Snopek, J. Orsavova Molecules. **22**, 944 (2017)
57. K. Kasprzak, T. Oniszczuk, A. Wojtowicz, M. Waksmundzka-Hajnos, M. Olech, R. Nowak, A. Oniszczuk, J. Anal. Methods Chem. **2018**, 7830546 (2018)
58. Z. Liang, H. Liang, Y. Guo, D. Yang, Int. J. Mol. Sci. **22**, 2261 (2021)
59. S. Lachowicz-Wiśniewska, I. Ochmian, J. Oszmiański, R. Wiśniewski, M. Bernatek, P. De Rubiński, Vita Pharmaceuticals. **18**, 674 (2025)
60. S.H. Nile, Y.S. Keum, A.S. Nile, S.S. Jalde, R.V. Patel, J. Biochem. Mol. Toxicol. **32**, e22002 (2018)
61. P. Lakhanpal, D.K. Rai, Internet J. Med. Update. **2**, 22–37 (2007)
62. L. Duysak, A. Ertürk, M. Becit-Kızılkaya, S. Apar, İ. Gülçin, ChemistrySelect 10, e07164 (2025)
63. I. Aprodu, C.L. Chitescu, L. Grigore-Gurgu, L. Dumitrașcu, Appl. Sci. **15**, 7070 (2025)
64. İ. Gülçin, Ö.İ. Küfrevioğlu, M. Oktay, M.E. Büyükokuroğlu, J. Ethnopharmacol. **90**(2–3), 205–215 (2004)
65. I.D. Ochmian, J. Grajkowski, M. Smolik, Not Bot. Horti Agrobot Cluj-Napoca. **40**(1), 253–260 (2012)
66. P. Denev, M. Kratchanova, M. Ciz, A. Lojek, O. Vasicek, P. Nedelcheva, D. Blazheva, R. Toshkova, E. Gardeva, L. Yossifova, P. Hyrsl, L. Vojtek, Food Chem. **157**, 37–44 (2014)
67. L. Li, P. Zhou, Y. Wang, Y. Pan, M. Chen, Y. Tian, H. Zhou, B. Yang, H. Meng, J. Zheng, Food Chem. **383**, 132410 (2022)
68. T. Benali, S. Bakrim, R. Ghchime, N. Benkhaira, N. El Omari, A. Balahbib, D. Taha, G. Zengin, M.M. Hasan, S. Bibi, A. Bouyahya, Biotechnol. Genet. Eng. Rev. **40**(4), 3408–3437 (2024)
69. H. Zhao, J. Dong, J. Lu, J. Chen, Y. Li, L. Shan, Y. Lin, W. Fan, G. Gu, J. Agric. Food Chem. **54**(19), 7277–7286 (2006)
70. A. Cvetanović, G. Zengin, Z. Zeković, J. Švarc-Gajić, S. Ražić, A. Damjanović, P. Mašković, M. Mitić, Food Chem. Toxicol. **121**, 458–466 (2018)
71. G. Zdunić, A.A. Aradski, D. Gođevac, J. Živković, S.D. Laušević, D.K. Milošević, K. Šavikin, Ind. Crops Prod. **148**, 112328 (2020)
72. E.S. Gürer, Ş. Yıldırım, Ü.M. Kocyigit, A. Berisha, S. Kaya, J. Mol. Struct. **1321**, 139893 (2025)
73. G. Tan, C. Gyllenhaal, D.D. Soejarto, Curr. Drug Targets. **7**(3), 265–277 (2006)
74. S.T. Asma, U. Acaroz, K. Imre, A. Morar, S.R.A. Shah, S.Z. Hussain, S. Ince, Cancers. **14**(24), 6203 (2022)
75. P. Quintero-Rincón, K. Caballero-Gallardo, J. Olivero-Verbel, Nat. Prod. Bioprospect. **15**(1), 25 (2025)
76. K. Owczarek, D. Sosnowska, D. Kajszczak, U. Lewandowska, J. Physiol. Pharmacol. **73**(2), 233–243 (2022)
77. E.S. Gürer, A. Altıntaş, Cumhuriyet Sci. J. **45**(3), 537–542 (2024)
78. Z. Yang, K.W. Chan, M.Z. Abu Bakar, X. Deng, Plants. **13**(17), 2492 (2024)
79. X. Deng, Z. Yang, K.W. Chan, N. Ismail, M Z. Abu Bakar Antioxid. **13**(9), 1030 (2024)
80. X. Deng, Z. Yang, K.W. Chan, M Z. Abu Bakar Pharm. **16**(8), 1011 (2024)
81. X. Deng, M.Y. Zanna, H. Ahmed, N. Ismail, K.W. Chan, N.M. Esa, Z. Yang, Mater. Res. Express. **12**, 072001 (2025)

Publisher's Note Springer Nature remains neutral with regard to jurisdictional claims in published maps and institutional affiliations.